Biosensors and Bioelectronics 87 (2017) 931–940

Contents lists available at ScienceDirect

Biosensors and Bioelectronics

journal homepage: www.elsevier.com/locate/bios

Quantum dots-labeled strip biosensor for rapid and sensitive detection of microRNA based on target-recycled nonenzymatic amplification strategy

Huaping Deng[a], Qianwen Liu[b,c,d,e], Xin Wang[b,c,d,e], Ru Huang[a], Hongxing Liu[a], Qiumei Lin[a], Xiaoming Zhou[a,*], Da Xing[a,*]

[a] MOE Key Laboratory of Laser Life Science & Institute of Laser Life Science, College of Biophotonics, South China Normal University, Guangzhou 510631, China
[b] Department of Thoracic Surgery, Sun Yat-Sen University Cancer Center, Guangzhou 510060, China
[c] Guangdong Esophageal Cancer Institute, Guangzhou 510060, China
[d] State Key Laboratory of Oncology in South China, Guangzhou 510060, China
[e] Collaborative Innovation Center of Cancer Medicine, Guangzhou 510060, China

ARTICLE INFO

Keywords:
MicroRNA detection
Strip biosensor
Quantum dots
Nonenzymatic amplification

ABSTRACT

MicroRNAs (miRNAs) have been proved to be potential biomarkers in early cancer diagnosis. It is of great significance for rapid and sensitive detection of miRNAs, particularly with point-of-care (POC) diagnosis. Herein, it is the first time to construct quantum dots (QDs)-labeled strip biosensor based on target-recycled nonenzymatic amplification strategy for miRNA detection. In the system, QDs were served as bright, photostable signal labels, which endow this biosensor with good detection efficiency. Moreover, a target-recycled amplification strategy relies on sequence-specific hairpins strand displacement process without the assistance of enzymes, was introduced to further improve the sensitivity. Meanwhile eliminating the requirement of environment-susceptible enzyme protein makes it easy to preserve and enhances the stability and reproducibility of this sensor. Benefiting from these outstanding characteristics, this platform exhibited a good detection sensitivity range from 2 fmol to 200 fmol with a limit of 200 amol, using only 20 μL of sample within 80 min. The assay was also 10-fold more sensitive than that with a conventional colloidal gold-based test strip for miRNA detection. Additionally, the analysis of miRNA in various tumor cell extracts was in accordance with the performance of quantitative realtime polymerase chain reaction (qRT-PCR). Clinical tumor samples were also tested, and 16 of 20 samples gave out positive signals, which demonstrated the practical application capacity of the biosensor. Therefore, the proposed biosensor holds great promise for potential POC applications and early cancer diagnosis.

1. Introduction

MicroRNAs (miRNAs) are small endogenous noncoding RNAs that act as important regulators of gene expression by mediating mRNA cleavage or translational repression (He and Hannon, 2004; Krol et al., 2010). And accumulative evidences indicated that miRNAs dysregulation and aberrant expressions are directly related to a variety of diseases, especially human cancers (Bartels and Tsongalis, 2009; He et al., 2005; Ventura and Jacks 2009). With a high clinic diagnostic value, miRNAs have been regarded as potential biomarkers for early cancer diagnostic which is very critical to improve the curative effectiveness and survival rate (Calin and Croce, 2006; Li et al., 2014). In spite of their great promise, the analysis of miRNAs still remains challenging due to their intrinsic characteristics such as short lengths, trace-amounts in biological samples and highly homologous sequences among family members (Iorio et al., 2005). Conventional methods involve northern blotting, quantitative reverse transcription polymerase chain reaction (qRT-PCR) and microarray technology, offer high accuracy and sensitivity also make great contributions to miRNAs analysis (Graybill and Bailey, 2016; Varallyay et al., 2008; Yin et al., 2008a). Nonetheless, they possess some limitations such as tedious procedure, lengthy assay time and much depending on laboratory-oriented sophisticated instruments, which severely hamper their further practical application (Cissell et al., 2007). Accordingly, it is highly desirable to develop a convenient, rapid and economical approach for miRNAs detection which could assist and hasten early cancer diagnosis, particularly under extremely resource-limited conditions.

In recent years, considerable efforts have been made toward developing point-of-care (POC) diagnostics, since it provides equip-

* Corresponding authors.
E-mail addresses: zhouxm@scnu.edu.cn (X. Zhou), xingda@scnu.edu.cn (D. Xing).

http://dx.doi.org/10.1016/j.bios.2016.09.043
Received 8 July 2016; Received in revised form 29 August 2016; Accepted 12 September 2016
Available online 12 September 2016
0956-5663/

ment-free, sensitive and robust diagnosis approach for accident points, emergency situations or somewhere low-resource settings (Gubala et al., 2012; Hartman et al., 2013; Peeling and Mabey, 2010). Likewise, paper-based biosensor, one of the most popular POC diagnostics format has received increasing concerns and holds great potential for further developing POC diagnostics, owing to its unique advantages of cost-effectiveness, small sample volume, speedy assay time and long-term stability (Hu et al., 2014; Parolo and Merkoci, 2013). Paper-based biosensor has been widely applied for numerous analytes detection containing proteins, nucleic acids, metal ions and so forth. (He et al., 2011; Lopez Marzo et al., 2013; Xu et al., 2014). Our group has also worked on developing paper-based platform for pathogenic bacteria and plant virus detection (Liu et al., 2014; Wei et al., 2014). However, to date, little attention has been paid on paper-based platform for miRNA detection (Gao et al., 2014; Yildiz et al., 2013). As a matter of fact, miRNAs can be unexpectedly well preserved in human blood serum and plasma (Iorio et al., 2005), which may enable them be adaptive for paper-based platform detection. Whereas in consideration of such low-abundant expression of miRNAs in biological samples, a high detection sensitivity should be required for miRNAs analysis (Volinia et al., 2006).

To address this concern, on one hand, the explorations of nanomaterials technology in the field of biosensors have opened up new opportunities for ameliorating the performance of paper-based biosensor (Quesada-González and Merkoçi 2015). The nanomaterials include colloidal gold nanoparticles (AuNPs), carbon nanotubes, QDs, up-converting phosphors and magnetic beads (Huang et al., 2016; Zhang et al., 2014). Among them, QDs, a kind of fluorescent semiconductor nanocrystals, exhibits unique optical properties and have gained increasing attention (Zhang et al., 2015). The superior brightness, robust photostability, broad excitation and size-tunable light emission spectra endow QDs with potential application prospect to be an ideal fluorescent labels for bioassays, bioimaging, bioconjugates and optical biosensors (Jun et al., 2013; Wang et al., 2014). More specifically, QDs is considered as the most promising biological label in paper-based assays (Yang et al., 2010). It is not only on account of the excellent brightness and strong stability against photobleaching compared with organic fluorescent dyes that can enhance sensitivity and prolong lifetime in its usage as labels (Geissler et al., 2010), but also the broad absorption spectra permitting effective excitation by low-cost and accessible light sources like light-emitting diodes or handheld ultraviolet (UV) lamps (Singh et al., 2016). Thereby, combining the advantages of QDs with paper-based biosensor would result in promotion of detection efficiency and reproducibility. In addition, QDs labeled the strip biosensor is the first time to introduce for miRNA detection.

On the other hand, a myriad of nucleic acid amplification strategies have been employed to detect miRNA for the high sensitivity and preferable specificity (Jia et al., 2010; Zhao et al., 2015). Most of these amplification methods require protein enzymes which are costly, susceptible to sensing environments and may produce false positive signals, also difficult in storage that would limit its wide applications in biosensors (Gerasimova and Kolpashchikov, 2014; Li et al., 2016; Shi et al., 2016). In comparison to protein enzyme-based amplification methods, nonenzymatic amplification approaches are independent of environment-susceptible and expensive enzymes and show great potential in POC diagnosis. Of particular interest is target-recycled nonenzymatic amplification approach, which was inspired by programming biomolecular self-assembly pathways (Cheglakov et al., 2015; Li et al., 2011). The target-recycled nonenzymatic amplification system consists of two rationally designed sequence-specific hairpin probes, relies on their hybridization and strand displacement process with the cyclic reuse of the target (Yin et al., 2008b). It is worthy to mention that, the target-recycled amplification method not only greatly enhances the detection sensitivity, the isothermal operation condition and no enzyme involved also makes the detection easy to preserve and thus guaranteeing better reproducibility. The favorable features render it to be well-suitable for combination of the strip biosensor assay.

Herein, we firstly proposed a robust and user-friendly QDs-labeled strip biosensing platform for visual, rapid and sensitive detection of miRNA, whereby taking full advantages of the unique optical properties of QDs and convenient performance of target-recycled nonenzymatic amplification strategy. And miRNA 21 (miR-21), a potential cancer biomarker that has been confirmed associated with lung adenocarcinoma and hepatocellular liver carcinoma (Kumarswamy et al., 2011), was selected to examine the performance of the proposed platform. Besides, the practical application capacity of the platform in real biological sample was also verified through analyzing miRNAs from four tumor cell lines. Attributed to the high sensitivity, rapid assay time and convenience of operation, our method may become a potential alternative tool for miRNA determination in biomedical research and early cancer diagnosis.

2. Experimental section

2.1. Materials and reagents

Quantum dots (λ_{ex}=605 nm) coated with streptavidin were synthesized by Wuhan Jiayuan Quantum Dots Co., Ltd. (Wuhan, China). An HM3020 X-Z two-dimensional dispenser and a GD300 Goldbio cutting module were purchased from Shanghai Goldbio Tech. Co., Ltd. (Shanghai, China). Cellulose fiber sample pads, conjugate pads, plastic adhesive backing pads, absorption pads and nitrocellulose membranes were purchased from Millipore (Billerica, MA). The RNAiso for small RNA and RNAase inhibitor were the products of Takara Biotechnology (Dalian) Co., Ltd. Gold(III) chloride trihydrate, bovine serum albumin (BSA) and Streptavidin were obtained from Sigma-Aldrich (St. Louis, MO, USA). Tris (2-carboxyethyl) phosphine hydrochloride (TCEP), tween-20, sodium chloride-sodium citrate (SSC) buffer (20×), phosphate buffered saline (PBS) buffer (20×) solution and the regents related to electrophoresis were purchased from Shanghai Sangon Biotechnology Co. Ltd. QRT-PCR primers, signal probes, capture probes and hairpin probes including biotinylated DNA probes were commercially synthesized and purified by Sangon Biotechnology Co. (Shanghai, China). Synthetic miRNAs were ordered from Invitrogen. All oligonucleotides were purified by ULTRAPAGE and their sequences were listed in Tables S1 and S2. When required, all chemical solutions and buffers were prepared in ultrapure water (18.2 MΩ/cm).

2.2. Preparation of hairpin probes

For the purpose of establishing the miRNA detection platform, hairpin probe 1 (H1) and hairpin probe 2 (H2) were carefully designed based on the principle of the nonenzymatic amplification strategy (Yin et al., 2008b). In addition, miR-21 was chosen as the target, whose sequence was taken into account. H2 was modified with biotin. Before the nonenzymatic amplification, both H1 and H2 were incubated in 1× PBS buffer and followed a gradient cooling process, which contained a denaturation at 95 °C for 5 min and a gradient cooling step that drops 5 degrees per minute until cooling down to the room temperature to ensure the probes were perfectly folded into a hairpin structure. Then the probes were stored at 4 °C for later use.

2.3. Preparation of QDs signal probes

For the preparation of QDs signal probes, we designed DNA probes modified with biotin at the 5′ terminus. Biotinylated DNA probes and QDs coated with streptavidin (QDs-605, 1 μM) were mixed at a molar ratio of 30:1 and the mixture was stirred gently for 30 min guaranteeing the streptavidin and biotin to bind completely. Then, to remove excess unbound biotinylated probes, the solution was centrifuged at 2000 rpm on a Nanosep 10 K OMEGA tubular ultrafiltration mem-

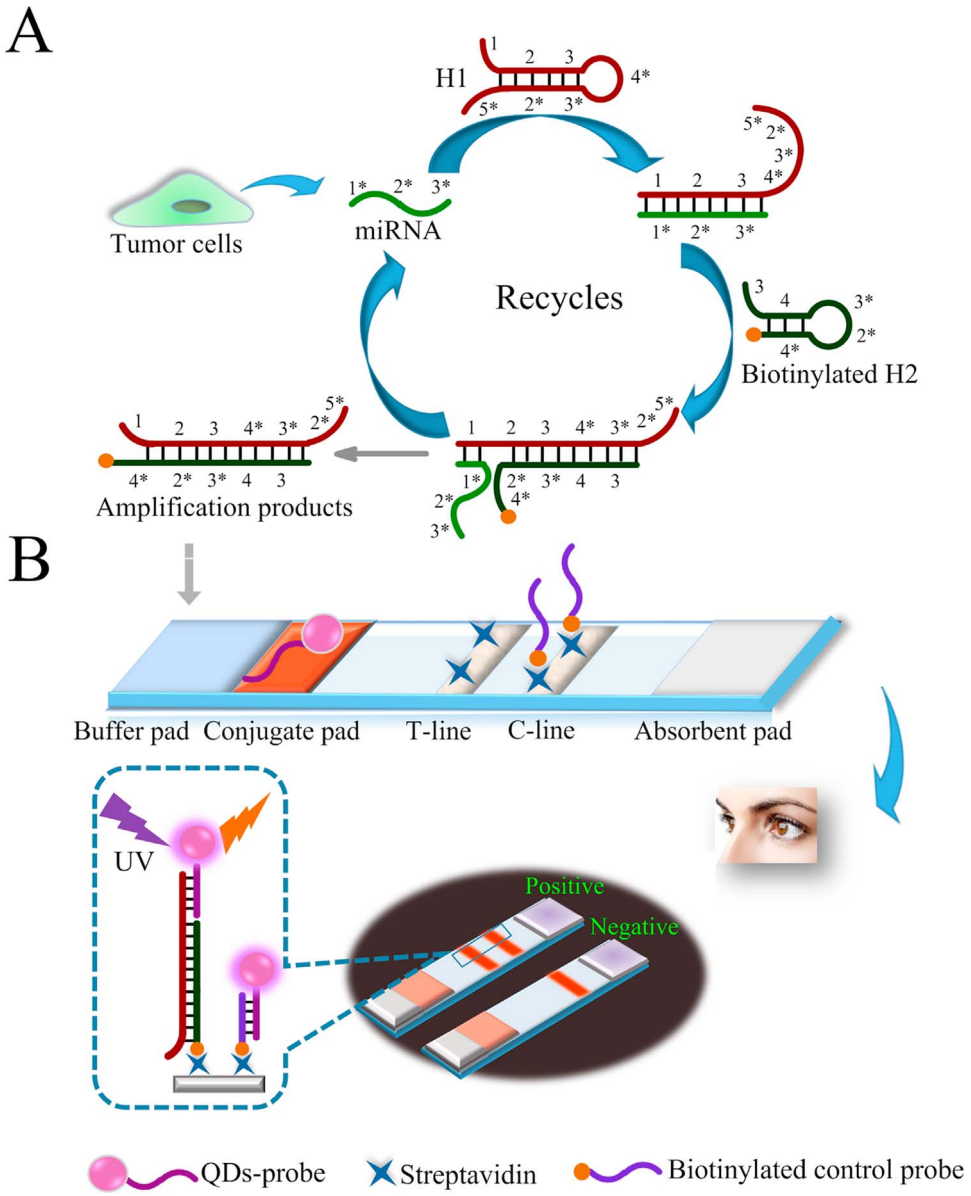

Fig. 1. (A) Principle of target-recycled nonenzymatic amplification and (B) schematic illustration of the QDs-labeled strip biosensor for the amplification products detection.

brane (Pall Corporation, Port Washington, NY). And washed with PBS buffer (1×), then the QDs signal probes were resuspended in a solution containing 20 mM Na_3PO_4, 5% BSA, 0.25% Tween-20%, and 10% sucrose, stored at 4 °C until future use. The characterization of QDs signal probes was shown in Fig. S1.

2.4. Assembly of the strip biosensor

The fabrication of the test strip was based on four major steps: (i) Preparing the buffer pad and conjugation pad which were made of glass fibers. 20 μL of the suspension solution containing 10 nM QDs was dispensed onto the conjugation pad, dried at room temperature, and then stored in a desiccator. (ii) The test line and control line were prepared by the HM3020 dispenser dispensing streptavidin and streptavidin-biotinylated capture probe onto the nitrocellulose (NC) membrane, respectively. The distance between the test line and control line was around 4 mm. The membrane was dried at room temperature and stored in a dry state. (iii) Assembly of the buffer pad, conjugate pad, NC membrane and absorbent pad onto plastic adhesive backing in an orderly manner with an overlap of 2 mm. (iv) The whole assembled plate with a 4 mm width was cut by the GD300 Goldbio cutting module and stored in a desiccator for the subsequent assays.

2.5. Cell culture and small RNA extraction

Human lung adenocarcinoma cells (A549), human cervical cancer cell lines (HeLa), human hepatocellular liver carcinoma cell lines (HepG2), human breast adenocarcinoma cells (MCF-7) and human umbilical vein endothelial cells (HUVEC) were cultured at 37 °C with 5% CO_2 and 95% air in a humidified incubator, and grown in Dulbecco's modified Eagle's medium (DMEM). The media were supplemented with 10% fetal bovine serum (FBS).

Total small RNA was isolated from five cell lines (HeLa, MCF-7, HepG2, A549 and HUVEC) using a commercial RNAiso for small RNA extracting kit. (TakaRa, China). Human umbilical vein endothelial cells (HUVEC) were chosen as the normal miRNA expression level control. All operations followed the kit protocol, and the obtained small RNA was quantified by measuring the optical density at 260 nm. Then diluted with RNase-free water and stored at −80 °C.

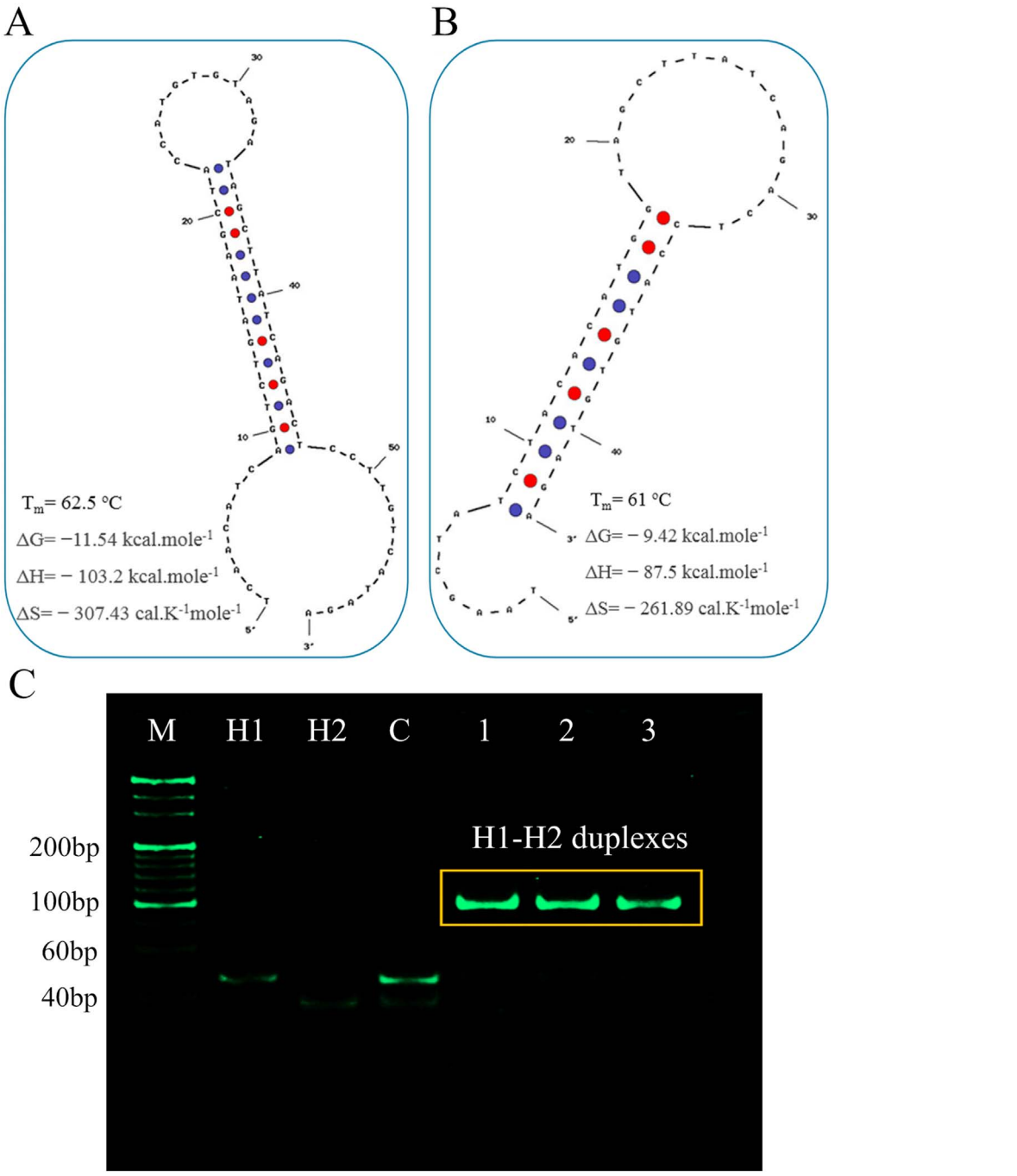

Fig. 2. (A) Planar construction and thermal kinetic parameters of H1 probe and (B) planar construction and thermal kinetic parameters of H2 probe. (C) 10% PAGE of nonenzymatic amplification products. M: DNA marker, H1: hairpin probe 1, H2: hairpin probe 2, C: negative control, lanes 1–3: three paralleled amplification experiments. The final concentration of miR-21, H1 and H2 were set as 10 nM, 150 nM and 100 nM, respectively.

2.6. Assay procedure with QDs-labeled strip biosensor

The whole procedure consists of a target-recycled nonenzymatic amplification and strip detection steps. The amplification procedure was performed by adding different concentrations miR-21 to a mixture with final reaction volume of 20 μL. The mixture contains H1 and H2 prepared in the previous step, 1× PBS buffer, RNAase inhibitor with a final concentration of 1 U/μL. RNAase inhibitor was used to protect the synthetic miR-21 from degradation by the RNAase in the environment. And the amplification system was carried out at 37 °C for 1 h. At the end of amplification procedure, the products were dispensed directly onto the NC membrane. After 10 min, the running buffer was dropped onto the buffer pad. As a result, QDs signal probes on the conjugate pad flowed through the reaction membrane under capillary action. Each sample test was repeated for three times under the same condition. 10 min later, the test strip was placed into the UV chamber or just under a handheld ultraviolet lamp which could provide with the 365 nm UV light excitation. Fluorescence intensity measurements were conducted by photographing the strip with a cell phone or digital camera and then determined the peak area of test line using ImageJ software.

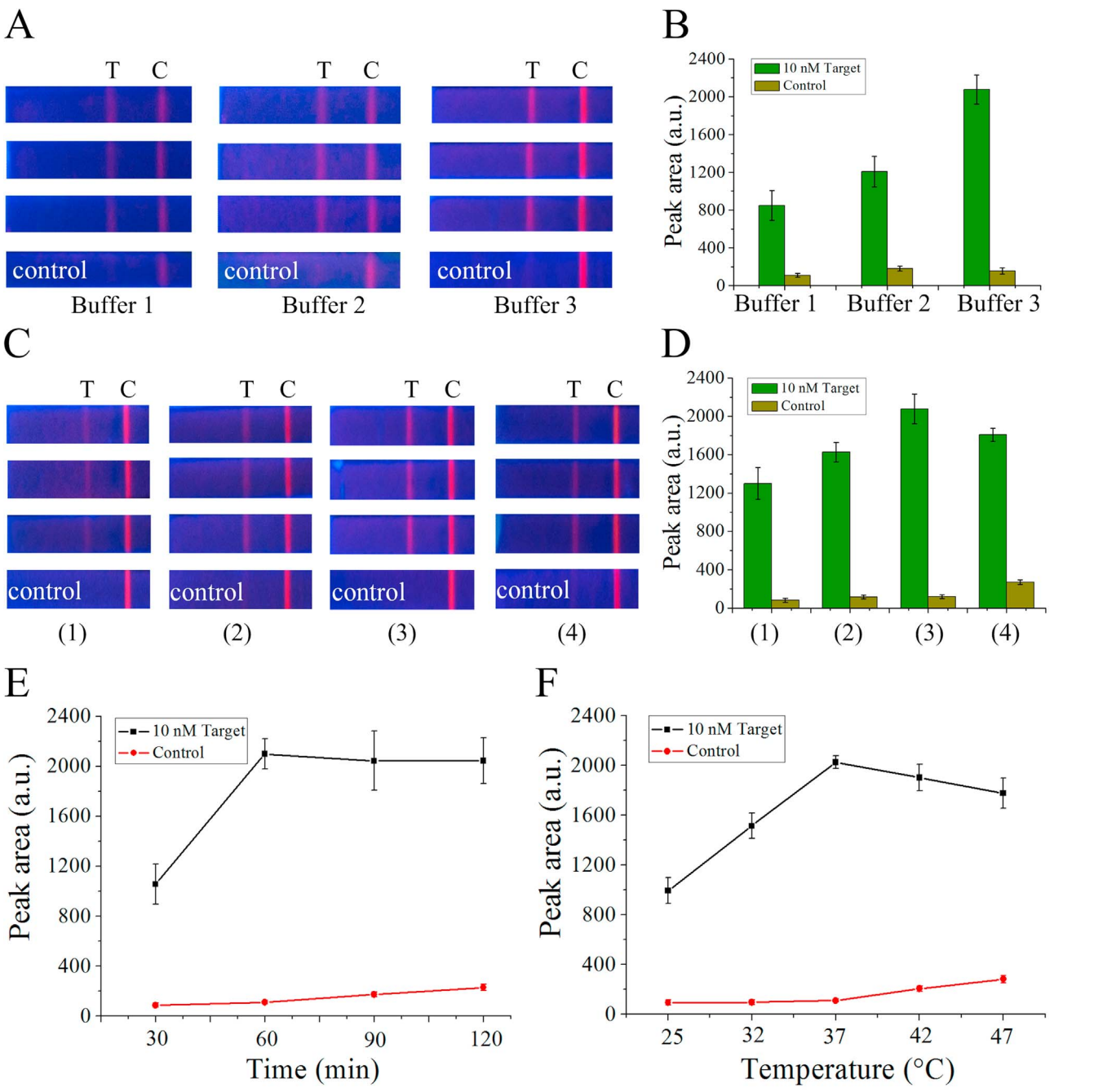

Fig. 3. Optimizations of experimental parameters. (A) Fluorescence photographs of QDs-based strip biosensor with different kinds of running buffers: (1) buffer1: PBST, (2) buffer2: PBST+SSC, (3) buffer3: PBST+SSC+1% BSA. (B) Histograms of the corresponding peak areas on the test lines of (A). (C) Fluorescence photographs of QDs-based strip biosensor for the responds with different ratios of H1 to H2: (1) 0.5:1; (2) 1:1; (3) 1.5:1; (4) 2:1. (D) Histograms of the peak areas on the test lines of (C). (E) Evaluation of the effect of incubating time (30–120 min). (F) Evaluation of the effect of incubating temperature (25–47 °C).

3. Results and discussion

3.1. Principle of the method

An overview of the QDs-labeled strip biosensor for miRNA detection based on target recycled nonenzymatic amplification strategy was schematically illustrated in Fig. 1. In detail, the overall concept of the target recycled amplification strategy was shown in Fig. 1A, which relies on two sequence-specific hairpin probes H1 and biotinylated H2. H1 comprises seven regions named as 1, 2, 3, 4*, 3*, 2*, 5*. The regions 1, 2, 3 are completely complementary with the target. Region 1 supports as the recognition domains to open up H1. The region 5* was designed for hybridizing with the signal probe. The biotinylated H2 contains five regions named as 3, 4, 3*, 2*, 4*. The region 3, 4, 3*, 2* were designed for complementary to H1 and region 3 provides the breakthrough to unfold H2. In the present of target miRNA, the stem of H1 would be unfolded, which resulted in exposing the concealed sequence of H1′s stem that is complementary to H2. With the interaction of H1 and H2, target miRNA released from H1-H2 duplexes and could be “recycled” leading to a new amplification circulation based on the strand displacement mechanism, which produced plenty of H1-H2 duplexes.

The visual detection of the amplification products on strip platform was shown in Fig. 1B. The amplification products H1-H2 duplexes were added directly to the NC membrane, and captured by streptavidin immobilized on the strip. Then QDs signal probes migrated along the

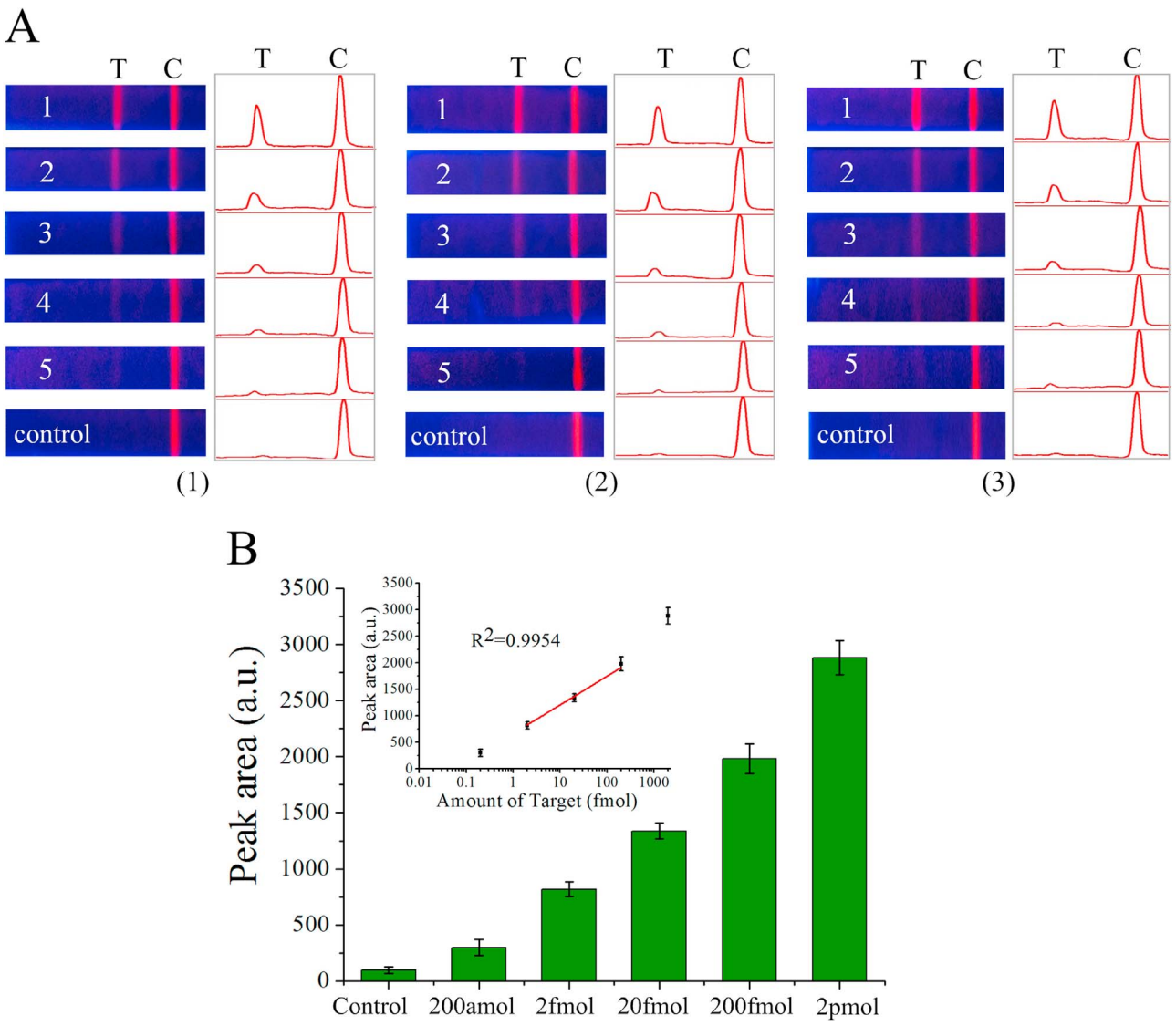

Fig. 4. Sensitivity assay of the QDs-based strip sensor for detection of miR-21. (A) Fluorescence photographs (left) and corresponding optical responses (right). Strips 1–5 correspond to amounts of 2 pmol, 200 fmol, 20 fmol, 2 fmol and 200 amol; strip C was a negative control. Panels 1–3 represent the results were repeated for the three times, respectively. (B) Histograms of the corresponding peak areas on the test lines of (A). Inset shows the calibration plot of the peak area of the test line versus miR-21 amounts.

NC membrane with the running buffer by capillary action and hybridized with the H1-H2 duplexes, which resulted in the accumulation of QDs on the test line. As the buffer continues migrating, the excess QDs signal probes hybridized with the control probe leading to the accumulation of QD on the control line. Under UV light excitation, the fluorescence of QDs both on the test line and the control line would be visualized. In the absence of target, H1 and H2 could not interact with each other to initiate the amplification reaction. As a result, there was no QDs fluorescence on the test line. The fluorescence of QDs on the control line would confirm the validity of the strip. Qualitative results were obtained simply by photographing the strip, and quantitative analysis was realized by recording the fluorescence intensity of the test line with ImageJ software.

3.2. Feasible analysis of the target-recycled nonenzymatic amplification strategy

In light of the target-recycled nonenzymatic amplification strategy as aforementioned, two sequence-specific hairpin probes were rationally designed and the structures were shown in Fig. 2A and B. The relevant parameters T_m (annealing temperature), ΔG (gibbs free energy), ΔH (enthalpy change) and ΔS (entropy change) of hairpin probes were calculated by Oligo Analyzer 3.1, respectively. By means of these parameters, the availability of the stem-loop structure designed would be estimated intuitively.

With the purpose of further confirmation the validities of the target-recycled nonenzymatic amplification strategy, 10 nM of miR-21 was amplified by the amplification system. The amplification products were detected by 10% polyacrylamide gel electrophoresis (PAGE) with the coloration of SYBR I and SYBR II. As can be seen from Fig. 2C, the bands of the amplification products H1-H2 duplexes were obvious, which demonstrates this amplification system was feasible.

3.3. Optimization of experimental parameters

For the sake of obtaining excellent analytical performance, different experimental conditions were systematically optimized. And the according control group was conducted respectively at the same condition. Running buffer plays an important role in performance of the strip detection platform, which would minimize nonspecific adsorption and increase the sensitivity and reproducibility. Therefore, three types of different running buffers were compared: buffer 1 was PBST, contains PBS (10 mM, pH 7.4) with Tween-20 at 0.05% (v/v); buffer 2 includes SSC and PBST; and buffer 3 was SSC and PBST supple-

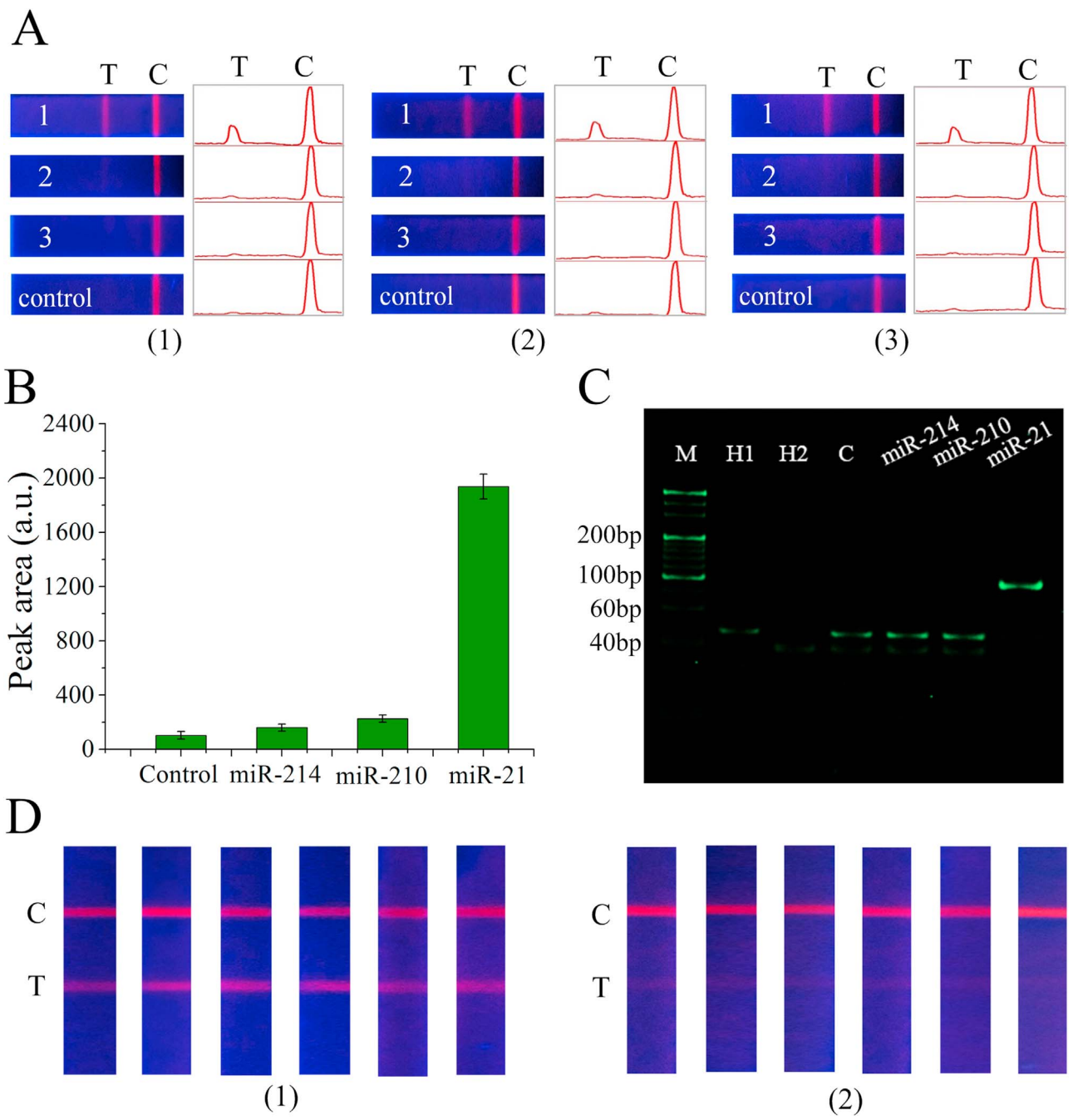

Fig. 5. Specificity and reproducibility evaluation of the QDs-based strip sensor for detection of miR-21: (A) Fluorescence photographs (left) and corresponding optical responses (right) for the specificity assay. Strip1: the result for the detection of miR-21; strip 2 and 3: the result for the detection of miR-210 and miR-214, respectively. Strip C: the negative control without target. Panels 1–3 represent the test was repeated for the three times. (B) Histograms of the peak areas on the test lines of (A). (C) 10% PAGE of the amplification results with different targets. (D) Fluorescence photographs from the reproducibility assay of QDs-labeled strip platform, (1) and (2) was performed with the target of 200 fmol and 200 amol, respectively.

mented with 1% of BSA fraction V (w/v). As shown in Fig. 3A and B, the QDs fluorescence intensity of test line with buffer 3 increased markedly, accordingly the control group in the absent of target decreased. Probably for that SSC buffer made contribution to the hybridization of nucleic acid, and BSA could reduce the nonspecific adsorption to improve the performance of the biosensor. Thereby buffer 3 was considered to be the optimum running buffer.

The ratio of H1 to H2 has significant effect on the amplification efficiency, which would facilitate the amplification procedure to yield more H1-H2 duplexes. Here, the effect of H1 to H2 ratio was studied by testing different H1 concentrations of 50 nM, 100 nM, 150 nM and 200 nM with a H2 concentration fixed at 100 nM. As shown in Fig. 3C and D, the QDs fluorescence intensity of the test line ascended with the augment concentration of H1. When the concentration of H1 reached 150 nM, the fluorescence intensity of the test line was strongest, and by contrast its control group was weaker. Therefore, the combination of 150 nM H1 to 100 nM H2 was used as the optimum for subsequent analytical purposes.

In order to further enhance the detection sensitivity, the incubating time and temperature were also optimized. The incubation time was evaluated ranging from 30 to 120 min. As the result depicted in Fig. 3E, the peak area of the test line elevated sharply when incubating time reached 60 min, and kept almost constant level thereafter. However, the control group maintained its increase along with increasing the

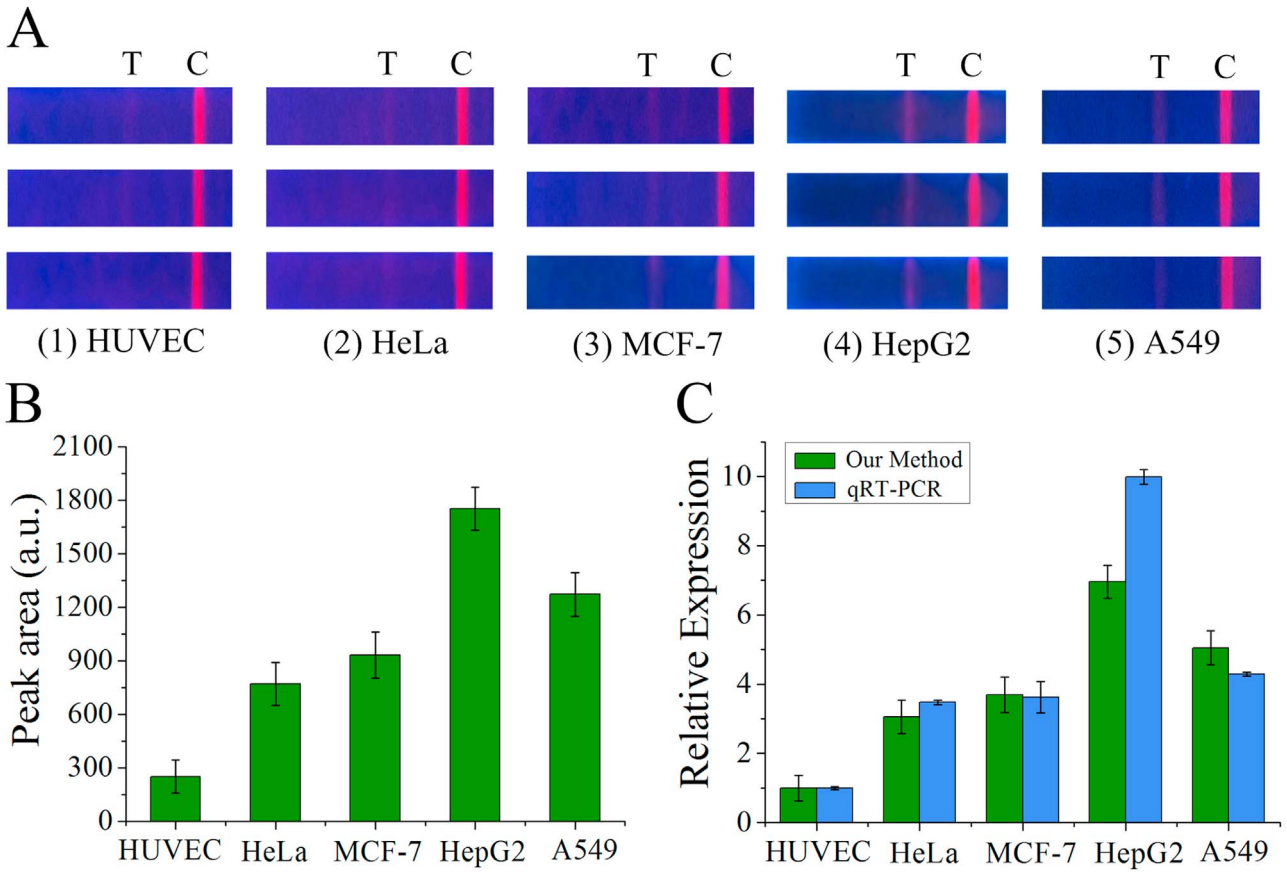

Fig. 6. Detection of miR-21 in cell lysate samples. (A) Fluorescence photographs of the strips for the triplicate test results from different cell samples. (B) Histograms of the peak areas of the test lines. (C) Representative relative expression levels of the miR-21 from different cell lines by our method and qRT-PCR. The expression level of miR-21 in human normal cell lines HUVEC was taken as a calibrator (set to 1) to calculate the relative expression levels in tumor cell lines.

incubation time. To obtain the maximal amplification efficiency, 60 min was chosen as the optimal incubation time. In addition, the incubating temperatures from 25 to 47 °C were selected to optimize (Fig. 3F). The peak area of test line increased gradually with the increase of incubation temperature at the early stage, and reached its maximum at 37 °C, then decreased. Conversely, the control group increased slowly as higher temperature would threaten the stability and integrality of hairpin probes. Therefore, 37 °C was employed as the optimum incubation temperature.

3.4. Sensitivity assay and comparison the proposed biosensor with AuNPs-based strip platform

Under the optimal experimental conditions, various amounts of standard miR-21 (varied from 200 amol to 2 pmol) were used to evaluate the sensitivity of the proposed platform. As shown in Fig. 4A, fluorescence photograph of the test strip could be observed clearly and the QDs fluorescence intensities decrease gradually with the reduction of miR-21. Through analysis the interrelated peak area of the test lines (see Fig. 4B) and based on three times the standard deviation corresponding to the blank sample detection, the detection limit of this sensor was estimated to be approximately 200 amol. And the inset showed a good linear relationship between the intensities of the test line (peak area) with the amounts of miR-21 ranging from 2 fmol to 200 fmol and R^2 value of 0.9954 was obtained.

Additionally, the traditional test strip method based on AuNPs as labels, was also performed with different amounts of miR-21 under optimal experimental conditions, to compare the detection sensitivity of the QDs-labeled strip biosensor. From the results shown in Fig. S2, it can be concluded that the detection limit of the AuNPs-based test strip was 2 fmol, while that of the QDs-labeled strip biosensor was achieved 200 amol. About 10-fold improvement of the sensitivity with the QDs-labeled strip biosensor was obtained than the AuNPs-based test strip, which should be attributed to the excellent optical properties of QDs. Hence, QDs, the promising fluorescent nanomaterial utilized in strip biosensor would be a prominent analytical platform and be sound basis for sensitive POC detection.

3.5. Specificity and reproducibility of the biosensor for miRNA detection

Specificity is another important quality index in evaluating performance for the platform, as it is a significant challenge for miRNA assays to accurately recognize a specific miRNA in the presence of other homologous miRNAs. In the current study, miR-210, miR-214, and miR-21 (sequences as Table S1) were respectively amplified by this platform with the isometric concentration of 10 nM. And corresponding results were obtained and shown in Fig. 5A and B. The QDs fluorescence signal was obviously observed in miR-21 experimental group, on the contrary, the other experimental groups of miR-210 and miR-214 gave out very weak QD fluorescence signals on test lines, almost same with the control group. The results were also validated by 10% PAGE (Fig. 5C), and indicates that our method has good specificity to clearly discriminate miR-21 from other miRNAs.

Reproducibility for miRNA detection in practical applications is of great importance. The reproducibility of the platform was investigated through measuring the target miR-21 at 200 amol and 200 fmol with 6 replicates, respectively. And similar responses could be obtained each time (see Fig. 5D). The relative standard deviation (RSD) values of optical responses were 2.9% and 3.2%, respectively, which confirmed

the satisfactory reproducibility of this detection platform.

3.6. Real sample analysis and miR-21 expression level comparisons of tumor cells

To further investigate the validity of this method in real sample analysis, the sensor was evaluated through measured miR-21 from five different human cell lines, including A549, HeLa, HepG2, MCF-7 and the normal cell line HUVEC. The cell samples were processed by using a commercial small-RNA extraction kit then the total small RNA quantified by measuring the optical density at 260 nm.

As shown in Fig. 6A, the QDs fluorescence intensities on the test lines of the four tumor cell lines were remarkably stronger than the human normal cell line HUVEC, which was employed as the normal expression control group. For quantitative analysis, the intensities of the test lines were estimated (see Fig. 6B), the results not only indicated the distinct miR-21 difference expression between human normal cells and tumor cells, but also demonstrated miR-21 different expression levels among the four tumor cell lines. It was also in good agreement with the previous reports of up-regulated expression of miR-21 in tumors (Liao et al., 2014). Moreover, the detection capability of the proposed method in real sample analysis was further evaluated by contrasting with qRT-PCR (see Figs. S2 and S3). In qRT-PCR experiment, U6 small nuclear RNA (snRNA) was employed as the universal endogenous control and the relative expression was calculated by the equation: Fold change $=2^{-\Delta\Delta Ct}$. The sequences of probes and details for qRT-PCR were listed in Tables S2 and S3. It was obviously to be found from Fig. 6C, the results of the two methods were in accordance. Further detection with clinical tumor tissues were also conducted (the results were showed in Supplementary material Fig. S5). All these experimental findings suggested that the proposed method may be capable of high-confidence miRNA detection in real biological samples and has a very promising prospect in POC diagnosis.

4. Conclusion

In summary, a QDs-labeled strip biosensor based on target recycling nonenzymatic amplification was developed for sensitive, rapid and visual detection of miRNAs. The proposed method employed QDs-labeled strip biosensor as signal giving-out platform and took advantage of the target recycling nonenzymatic amplification reaction to further enhance the sensitivity, as a result, the satisfying detection limit of 200 amol was achieved within 80 min (including amplification process). What is more, miRNAs from four tumor cell lines were analyzed through the platform. In contrast to current methods for miRNA detection (see Table S4), our method exhibited remarkable advantages, particularly from the standpoint of POC diagnosis. It was not only simple and convenient operation eliminating the requirement for sophisticated equipment, but also rapid and sensitive analysis for qualitative (visual) and quantitative (optical responses of the test line) results. With reliance on the excellent performance proposed above, the platform can open the way for potential application in a wider range of fields, for instance, be extended to multiplexed detection of miRNA or other nucleic acid assay in POC; and developed to be a rapid miRNA detection kit.

Acknowledgments

This work was supported by the National Natural Science Foundation of China [21475048], the National Science Fund for Distinguished Young Scholars of Guangdong Province [2014A030306008], the Project of Guangzhou Science and Technology Plan [201508020003], and the Program of the Pearl River Young Talents of Science and Technology in Guangzhou [2013J2200021], the Special Support Program of Guangdong Province (2014TQ01R599), and the Outstanding Young Teacher Training Program of Guangdong Province (HS2015004).

Appendix A. Supplementary material

Supplementary data associated with this article can be found in the online version at doi:10.1016/j.bios.2016.09.043.

References

Bartels, C.L., Tsongalis, G.J., 2009. MicroRNAs: novel biomarkers for human cancer. Clin. Chem. 55 (4), 623–631.
Calin, G.A., Croce, C.M., 2006. MicroRNA signatures in human cancers. Nat. Rev. Cancer 6 (11), 857–866.
Cheglakov, Z., Cronin, T.M., He, C., Weizmann, Y., 2015. Live cell microRNA imaging using cascade hybridization reaction. J. Am. Chem. Soc. 137 (19), 6116–6119.
Cissell, K.A., Shrestha, S., Deo, S.K., 2007. MicroRNA detection: challenges for the analytical chemist. Anal. Chem. 79 (13), 4754–4761.
Gao, X., Xu, H., Baloda, M., Gurung, A.S., Xu, L.P., Wang, T., Zhang, X., Liu, G., 2014. Visual detection of microRNA with lateral flow nucleic acid biosensor. Biosens. Bioelectron. 54, 578–584.
Geissler, D., Charbonniere, L.J., Ziessel, R.F., Butlin, N.G., Lohmannsroben, H.G., Hildebrandt, N., 2010. Quantum dot biosensors for ultrasensitive multiplexed diagnostics. Angew. Chem. Int. Ed. 49 (8), 1396–1401.
Gerasimova, Y.V., Kolpashchikov, D.M., 2014. Enzyme-assisted target recycling (EATR) for nucleic acid detection. Chem. Soc. Rev. 43 (17), 6405–6438.
Graybill, R.M., Bailey, R.C., 2016. Emerging biosensing approaches for microRNA analysis. Anal. Chem. 88 (1), 431–450.
Gubala, V., Harris, L.F., Ricco, A.J., Tan, M.X., Williams, D.E., 2012. Point of care diagnostics: status and future. Anal. Chem. 84 (2), 487–515.
Hartman, M.R., Ruiz, R.C., Hamada, S., Xu, C., Yancey, K.G., Yu, Y., Han, W., Luo, D., 2013. Point-of-care nucleic acid detection using nanotechnology. Nanoscale 5 (21), 10141–10154.
He, L., Hannon, G.J., 2004. MicroRNAs: small RNAs with a big role in gene regulation. Nat. Rev. Genet. 5 (7), 522–531.
He, L., Thomson, J.M., Hemann, M.T., Hernando-Monge, E., Mu, D., Goodson, S., Powers, S., Cordon-Cardo, C., Lowe, S.W., Hannon, G.J., Hammond, S.M., 2005. A microRNA polycistron as a potential human oncogene. Nature 435 (7043), 828–833.
He, Y., Zhang, S., Zhang, X., Baloda, M., Gurung, A.S., Xu, H., Zhang, X., Liu, G., 2011. Ultrasensitive nucleic acid biosensor based on enzyme-gold nanoparticle dual label and lateral flow strip biosensor. Biosens. Bioelectron. 26 (5), 2018–2024.
Hu, J., Wang, S., Wang, L., Li, F., Pingguan-Murphy, B., Lu, T.J., Xu, F., 2014. Advances in paper-based point-of-care diagnostics. Biosens. Bioelectron. 54, 585–597.
Huang, X., Aguilar, Z.P., Xu, H., Lai, W., Xiong, Y., 2016. Membrane-based lateral flow immunochromatographic strip with nanoparticles as reporters for detection: a review. Biosens. Bioelectron. 75, 166–180.
Iorio, M.V., Ferracin, M., Liu, C.G., Veronese, A., Spizzo, R., Sabbioni, S., Magri, E., Pedriali, M., Fabbri, M., Campiglio, M., Menard, S., Palazzo, J.P., Rosenberg, A., Musiani, P., Volinia, S., Nenci, I., Calin, G.A., Querzoli, P., Negrini, M., Croce, C.M., 2005. MicroRNA gene expression deregulation in human breast cancer. Cancer Res. 65 (16), 7065–7070.
Jia, H., Li, Z., Liu, C., Cheng, Y., 2010. Ultrasensitive detection of microRNAs by exponential isothermal amplification. Angew. Chem. Int. Ed. 49 (32), 5498–5501.
Jun, H.K., Careem, M.A., Arof, A.K., 2013. Quantum dot-sensitized solar cells—perspective and recent developments: a review of Cd chalcogenide quantum dots as sensitizers. Renew. Sustain. Energy Rev. 22, 148–167.
Krol, J., Loedige, I., Filipowicz, W., 2010. The widespread regulation of microRNA biogenesis, function and decay. Nat. Rev. Genet. 11 (9), 597–610.
Kumarswamy, R., Volkmann, I., Thum, T., 2011. Regulation and function of miRNA-21 in health and disease. RNA Biol. 8 (5), 706–713.
Li, B., Ellington, A.D., Chen, X., 2011. Rational, modular adaptation of enzyme-free DNA circuits to multiple detection methods. Nucleic Acids Res. 39 (16), e110.
Li, J., Tan, S., Kooger, R., Zhang, C., Zhang, Y., 2014. MicroRNAs as novel biological targets for detection and regulation. Chem. Soc. Rev. 43 (2), 506–517.
Li, X., Peng, Y., Chai, Y., Yuan, R., Xiang, Y., 2016. A target responsive aptamer machine for label-free and sensitive non-enzymatic recycling amplification detection of ATP. Chem. Commun. 52 (18), 3673–3676.
Liao, Y., Huang, R., Ma, Z., Wu, Y., Zhou, X., Xing, D., 2014. Target-triggered enzyme-free amplification strategy for sensitive detection of microrna in tumor cells and tissues. Anal. Chem. 86 (9), 4596–4604.
Liu, H., Zhan, F., Liu, F., Zhu, M., Zhou, X., Xing, D., 2014. Visual and sensitive detection of viable pathogenic bacteria by sensing of RNA markers in gold nanoparticles based paper platform. Biosens. Bioelectron. 62, 38–46.
Lopez Marzo, A.M., Pons, J., Blake, D.A., Merkoci, A., 2013. High sensitive gold-nanoparticle based lateral flow immunodevice for Cd^{2+} detection in drinking waters. Biosens. Bioelectron. 47, 190–198.
Parolo, C., Merkoci, A., 2013. Paper-based nanobiosensors for diagnostics. Chem. Soc. Rev. 42 (2), 450–457.
Peeling, R., Mabey, D., 2010. Point-of-care tests for diagnosing infections in the developing world. Clin. Microbiol. Infect. 16 (8), 1062–1069.
Quesada-González, D., Merkoçi, A., 2015. Nanoparticle-based lateral flow biosensors. Biosens. Bioelectron. 73, 47–63.
Shi, K., Dou, B., Yang, J., Yuan, R., Xiang, Y., 2016. Cascaded strand displacement for non-enzymatic target recycling amplification and label-free electronic detection of

microRNA from tumor cells. Anal. Chim. Acta 916, 1–7.
Singh, G., Fisch, M., Kumar, S., 2016. Emissivity and electrooptical properties of semiconducting quantum dots/rods and liquid crystal composites: a review. Rep. Prog. Phys. 79 (5), 056502.
Varallyay, E., Burgyan, J., Havelda, Z., 2008. MicroRNA detection by northern blotting using locked nucleic acid probes. Nat. Protoc. 3 (2), 190–196.
Ventura, A., Jacks, T., 2009. MicroRNAs and cancer: short RNAs go a long way. Cell 136 (4), 586–591.
Volinia, S., Calin, G.A., Liu, C.G., Ambs, S., Cimmino, A., Petrocca, F., Visone, R., Iorio, M., Roldo, C., Ferracin, M., Prueitt, R.L., Yanaihara, N., Lanza, G., Scarpa, A., Vecchione, A., Negrini, M., Harris, C.C., Croce, C.M., 2006. A microRNA expression signature of human solid tumors defines cancer gene targets. Proc. Nat. Acad. Sci. USA 103 (7), 2257–2261.
Wang, D.-C., Hu, L.-H., Zhou, Y.-H., Huang, Y.-T., Li, X., Zhu, J.-J., 2014. Dual channel sensitive detection of hsa-miR-21 based on rolling circle amplification and quantum dots tagging. J. Biomed. Nanotechnol. 10 (4), 615–621.
Wei, J., Liu, H., Liu, F., Zhu, M., Zhou, X., Xing, D., 2014. Miniaturized paper-based gene sensor for rapid and sensitive identification of contagious plant virus. ACS Appl. Mater. Interfaces 6 (24), 22577–22584.
Xu, H., Chen, J., Birrenkott, J., Zhao, J.X., Takalkar, S., Baryeh, K., Liu, G., 2014. Gold-nanoparticle-decorated silica nanorods for sensitive visual detection of proteins. Anal. Chem. 86 (15), 7351–7359.
Yang, H., Li, D., He, R., Guo, Q., Wang, K., Zhang, X., Huang, P., Cui, D., 2010. A novel quantum dots-based point of care test for syphilis. Nanoscale Res. Lett. 5 (5), 875–881.
Yildiz, U.H., Alagappan, P., Liedberg, B., 2013. Naked eye detection of lung cancer associated miRNA by paper based biosensing platform. Anal. Chem. 85 (2), 820–824.
Yin, J.Q., Zhao, R.C., Morris, K.V., 2008a. Profiling microRNA expression with microarrays. Trends Biotechnol. 26 (2), 70–76.
Yin, P., Choi, H.M., Calvert, C.R., Pierce, N.A., 2008b. Programming biomolecular self-assembly pathways. Nature 451 (7176), 318–322.
Zhang, P., Zhuo, Y., Chang, Y., Yuan, R., Chai, Y., 2015. Electrochemiluminescent graphene quantum dots as a sensing platform: a dual amplification for microRNA assay. Anal. Chem. 87 (20), 10385–10391.
Zhang, P., Liu, X., Wang, C., Zhao, Y., Hua, F., Li, C., Yang, R., Zhou, L., 2014. Evaluation of up-converting phosphor technology-based lateral flow strips for rapid detection of Bacillus anthracis Spore, Brucella spp., and Yersinia pestis. PloS One 9 (8), e105305.
Zhao, Y., Chen, F., Li, Q., Wang, L., Fan, C., 2015. Isothermal amplification of nucleic acids. Chem. Rev. 115 (22), 12491–12545.